ASYMPTOTIC AND EXACT RADIATION BOUNDARY CONDITIONS FOR TIME-DEPENDENT SCATTERING

Lonny L. Thompson [*]
Department of Mechanical Engineering
Clemson University
Clemson, South Carolina, 29634
Email: lonny.thompson@ces.clemson.edu

Runnong Huan
Department of Mechanical Engineering
Clemson University
Clemson, South Carolina, 29634

ABSTRACT

Asymptotic and exact local radiation boundary conditions first derived by Hagstrom and Hariharan are reformulated as an auxiliary Cauchy problem for linear first-order systems of ordinary equations on the boundary for each harmonic on a circle or sphere in two- or three-dimensions, respectively. With this reformulation, the resulting radiation boundary condition involves first-order derivatives only and can be computed efficiently and concurrently with standard semi-discrete finite element methods for the near-field solution without changing the banded/sparse structure of the finite element equations. In 3D, with the number of equations in the Cauchy problem equal to the mode number, this reformulation is exact. If fewer equations are used, then the boundary conditions form uniform asymptotic approximations to the exact condition. Furthermore, using this approach, we formulate accurate radiation boundary conditions for the two-dimensional unbounded problem on a circle. Numerical studies of time-dependent radiation and scattering are performed to assess the accuracy and convergence properties of the boundary conditions when implemented in the finite element method. The results demonstrate that the new formulation has dramatically improved accuracy and efficiency for time domain simulations compared to standard boundary treatments.

INTRODUCTION

When modeling radiation from structures in an acoustic medium which extends to infinity with a domain based computational method such as the finite element method, the far-field is truncated at an artificial boundary surrounding the source of radiation. The impedance of the far-field is then represented on this boundary by either radiation boundary conditions, infinite elements, or absorbing sponge layers. Survey articles of various boundary treatments are given in (Tsynkov, 1998). If accurate boundary treatments are used, the finite computational region can be reduced so that the truncation boundary is relatively close to the radiator, and fewer elements than otherwise would be possible may be used, resulting in considerable savings in both cpu time and memory. In the frequency domain, several accurate and efficient methods for representing the impedance of the far-field are well understood, including the Dirichlet-to-Neumann (DtN) map (Keller, 1989; Grote, 1995a), and infinite elements (Burnett, 1994; Astley, 1998). However, efficient evaluation of accurate boundary treatments for the time-dependent wave equation on unbounded spatial domains has long been an obstacle for the development of reliable solvers for time domain simulations. Ideally, the artificial boundary would be placed as close as possible to the source, and the radiation boundary treatment would be capable of arbitrary accuracy at a cost and memory not exceeding that of the interior solver.

A standard approach is to apply local (differential) boundary operators which annihilate leading terms in the radial multipole expansion for outgoing wave solutions. A well known sequence of boundary conditions developed for a spherical truncation boundary are the local operators derived by Bayliss and Turkel (Bayliss, 1980). However, these and other approximate local boundary conditions exhibit significant spurious reflection for high-order wave harmonics, especially as the position of the

[*] Corresponding author.

truncation boundary approaches the source of radiation (Pinsky, 1991; Pinsky, 1992).

In recent years, new boundary treatments have been developed which dramatically improve both the accuracy and efficiency of time domain simulations compared to approximate local radiation boundary conditions. In (Grote, 1995b; Grote, 1996), exact nonreflecting boundary conditions (NRBC) are derived involving solution of an auxiliary Cauchy problem for linear first-order systems of time-dependent differential equations on a spherical boundary for each harmonic. In (Thompson, 1999a), this NRBC is rederived based on direct application of a result given in Lamb (Lamb, 1916), with improved scaling of the first-order system of equations associated with the NRBC. Formulation of the NRBC in standard semidiscrete finite element methods with several alternative implicit and explicit time-integrators is reported in (Thompson, 1999a; Thompson, 1999b). In (Thompson, 1999b), a modified version of the exact NRBC first derived in (Grote, 1996), is implemented in a finite element formulation. In order to obtain a symmetric system, the NRBC is reformulated with additional auxiliary variables on the truncation boundary. The modified version may be viewed as an extension of the second-order local boundary operator derived by Bayliss and Turkel (Bayliss, 1980), and gives improved accuracy when only a few harmonics are included in the spherical expansion/transformation. In (Thompson, 1999c), a method is described for calculating far field solutions concurrently with the near-field solution based on the exact NRBC. At each discrete time step, radial modes computed on a spherical artificial boundary which drive the exact NRBC for the near-field solution, are imposed concurrently as data for the radial wave equation in the far-field. The radial grid is truncated at the far-field point of interest with the modal form of the exact NRBC. The solution in the far-field is then computed from an inverse spherical harmonic transform of the radial modes.

Hagstrom and Hariharan (Hagstrom, 1998) have derived a sequence of radiation boundary conditions involving first-order differential equations in time and tangential derivatives of auxiliary functions on a circular or spherical boundary. They indicate how these local conditions may be effectively implemented in a finite difference scheme using only local tangential operators, but at the cost of introducing a large number of auxiliary functions at the boundary. Numerical experiments were conducted for a model problem involving the Fourier modes of the wave equation in two-dimensions using a finite difference method. However, direct finite element implementation of this sequence in a standard Galerkin variational equation would result in a nonsymmetric system of equations.

In this paper we rederive the sequence of local boundary conditions described in (Hagstrom, 1998) in terms of harmonics and reformulate the recursive equations as a Cauchy problem involving systems of first-order ordinary differential equations on the boundary, similar to that used in (Grote, 1995b;
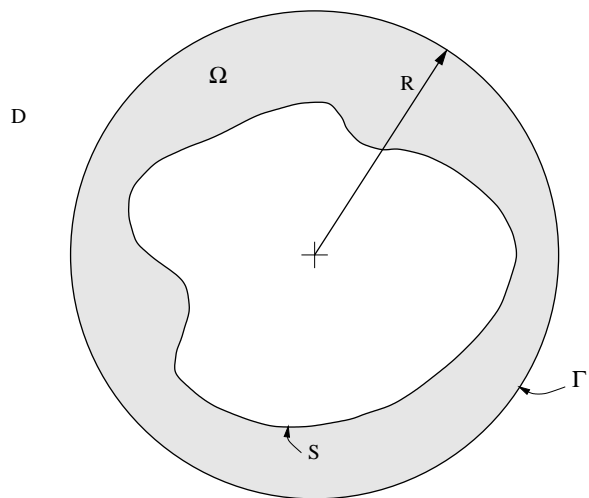

Figure 1. ILLUSTRATION OF UNBOUNDED REGION $R \subset R^d$ SURROUNDING A SCATTERER S. THE COMPUTATIONAL DOMAIN $\Omega \subset R$ IS SURROUNDED BY A TRUNCATION BOUNDARY Γ OF RADIUS R, WITH EXTERIOR REGION $D = R - \Omega$.

Thompson, 1999a). A modified version similar to the formulation given in (Thompson, 1999b) is also reported. The reformulation is based on the hierarchy of local boundary operators used by Bayliss and Turkel which satisfy truncations of the multipole expansion for each harmonic and a recursion relation for the expansion coefficients. With this reformulation, the resulting radiation boundary conditions involves first-order derivatives only, and as a result, may be implemented efficiently with standard semidiscrete finite element methods without changing the symmetric and banded/sparse structure of the matrix equations.

INITIAL-BOUNDARY VALUE PROBLEM

We consider time-dependent scattering and radiation of waves in an infinite d-dimensional region $R \subset R^d$, surrounding an object with surface S. For computation, the unbounded region R is truncated by an artificial boundary Γ. We assume that the hypersurface Γ is a d-dimensional ball of radius $\parallel \boldsymbol{x} \parallel = R$, i.e., a sphere in three-dimensions ($d = 3$), or a circle in two-dimensions ($d = 2$). We then denote by $\Omega \subset R$, the finite subdomain bounded by $\partial\Omega = \Gamma \cup S$, see Figure 1.

Within Ω, the solution $\phi(\boldsymbol{x},t) : \Omega \times [0,T] \mapsto R$, satisfies the scalar wave equation,

$$\frac{1}{c^2}\frac{\partial^2 \phi}{\partial t^2} = \nabla^2 \phi + f(\boldsymbol{x},t), \qquad \boldsymbol{x} \in \Omega,\, t \in [0,T] \qquad (1)$$

2

with initial conditions,

$$\phi(\boldsymbol{x},0) = \phi_o(\boldsymbol{x}), \qquad \dot{\phi}(\boldsymbol{x},0) = \dot{\phi}_o(\boldsymbol{x}), \qquad \boldsymbol{x} \in \Omega \qquad (2)$$

and driven by the time-dependent radiation boundary condition on the surface S:

$$\beta_1 \frac{\partial \phi}{\partial n} + \beta_2 \frac{\partial \phi}{\partial t} + \gamma \phi = g(\boldsymbol{x},t), \qquad \boldsymbol{x} \in S, \ t \in [0,T] \qquad (3)$$

The wave speed c, and β_1, β_2, γ are real, and we assume $c > 0$, and $\beta_1, \beta_2 \geq 0$. The source f and initial data ϕ_o and $\dot{\phi}_o$ are assumed to be confined to the computational domain Ω, so that in the exterior region $D = R - \Omega$, i.e., the infinite region outside Γ, the scalar field $\phi(\boldsymbol{x},t)$ satisfies the homogeneous form of the wave equation,

$$\frac{1}{c^2} \frac{\partial^2 \phi}{\partial t^2} = \nabla^2 \phi, \qquad \boldsymbol{x} \in D, \ t \in [0,T] \qquad (4)$$

$$\phi(\boldsymbol{x},0) = 0, \qquad \dot{\phi}(\boldsymbol{x},0) = 0, \qquad \boldsymbol{x} \in \Omega \qquad (5)$$

In the following, we introduce polar and spherical coordinates $(r, \boldsymbol{\theta})$, where $\boldsymbol{\theta} = \theta$ in two-dimensions and $\boldsymbol{\theta} = (\theta, \varphi)$ in three-dimensions, respectively, such that the wave equation can be written in separable form,

$$\frac{1}{c^2} \frac{\partial^2 \phi}{\partial t^2} = \frac{\partial^2 \phi}{\partial r^2} + \frac{2\alpha}{r} \frac{\partial \phi}{\partial r} + \frac{1}{r^2} \Delta_\Gamma \phi \qquad (6)$$

where

$$\Delta_\Gamma \phi = \begin{cases} \dfrac{\partial^2}{\partial \theta^2}, & d = 2 \\ \dfrac{1}{\sin \theta} \dfrac{\partial}{\partial \theta} \left(\sin \theta \dfrac{\partial \phi}{\partial \theta} \right) + \dfrac{1}{\sin^2 \theta} \dfrac{\partial^2 \phi}{\partial \varphi^2}, & d = 3 \end{cases} \qquad (7)$$

In the above, we have introduced the scaled dimensional value $\alpha = (d-1)/2$, such that

$$\alpha = \begin{cases} 1/2, & d = 2 \\ 1, & d = 3 \end{cases} \qquad (8)$$

The general solution to (6) is given by the expansion,

$$\phi(r,\theta,\varphi,t) = \sum_{n=n_0}^{\infty} \sum_{m=-m_0}^{m_0} \phi_{nm}(r,t) \, y_{nm}(\boldsymbol{\theta}) \qquad (9)$$

$$n_0 = \begin{cases} -\infty, & d = 2 \\ 0, & d = 3 \end{cases} \qquad (10)$$

$$m_0 = \begin{cases} 0, & d = 2 \\ n, & d = 3 \end{cases} \qquad (11)$$

and where y_{nm} are orthogonal harmonics normalized on Γ:

$$y_{nm}(\boldsymbol{\theta}) = \begin{cases} \dfrac{1}{\sqrt{2\pi R}} \exp(in\theta), & d = 2 \\ \sqrt{\dfrac{(2n+1)(n-|m|)!}{4\pi R^2 (n+|m|)!}} P_n^{|m|}(\cos \theta) \exp(im\varphi), & d = 3 \end{cases} \qquad (12)$$

The time-dependent modes $\phi_{nm}(r,t)$, $r \geq R$, $t \geq 0$ satisfy the radial wave equation,

$$\frac{1}{c^2} \frac{\partial^2 \phi_{nm}}{\partial t^2} = \left[\frac{\partial^2}{\partial r^2} + \frac{2\alpha}{r} \frac{\partial}{\partial r} - \frac{n(n+2\alpha-1)}{r^2} \right] \phi_{nm} \qquad (13)$$

$$\phi_{nm}(r,0) = 0, \qquad \dot{\phi}_{nm}(r,0) = 0, \qquad r \geq R \qquad (14)$$

For outgoing waves, the solution to (13) may be represented by the multipole expansion:

$$\phi_{nm}(r,t) = \sum_{k=0}^{K} r^{-k-\alpha} \phi_{nm}^k(r - ct) \qquad (15)$$

where

$$K = \begin{cases} \infty, & d = 2 \\ n, & d = 3 \end{cases} \qquad (16)$$

Substituting (15) into (13), we obtain the recursion relation for the expansion coefficients:

$$\left(\phi_{nm}^k \right)' = c_n^k \phi_{nm}^{k-1} \qquad (17)$$

where

$$c_n^k = \begin{cases} \dfrac{(k-1/2)^2 - n^2}{2k}, & d = 2 \\ \dfrac{k(k-1) - n(n+1)}{2k}, & d = 3 \end{cases} \qquad (18)$$

3

Construction of Radiation Boundary Conditions

In the following, we derive high-order accurate radiation boundary conditions suitable for numerical implementation, based on the hierarchy of local operators used by Bayliss and Turkel (Bayliss, 1980) which annihilate radial terms in the expansion (15). The local operators are easily constructed using a product of radial derivatives:

$$B_j = L_j(L_{j-1}(\cdots(L_2(L_1)))) \qquad (19)$$

$$L_j = \left(\frac{1}{c}\frac{\partial}{\partial t} + \frac{\partial}{\partial r} + \frac{2(j-1)+\alpha}{r}\right) \qquad (20)$$

However, the product form $B_p\phi_{nm}$, involves high order radial derivatives which limits the order j, which can be practically used in a numerical method. Inspired by the local boundary conditions of Hagstrom and Hariharan (Hagstrom, 1998), involving a sequence of first-order equations in time with tangential derivatives, we reformulate the Bayliss and Turkel boundary operators as a recursive sequence involving first-order time derivatives only for each mode. This sequence is then cast as a system of first-order differential equations in time, for each harmonic, which may be solved concurrently with the finite element equations.

In the following, we interpret the remainders of the Bayliss and Turkel operators (19) acting on the multipole expansion (15) as a sequence of functions with reduced radial order. We apply $B_1 = L_1$ to the radial expansion (15), with the result,

$$B_1\phi_{nm} = \left(\frac{1}{c}\frac{\partial}{\partial t} + \frac{\partial}{\partial r} + \frac{\alpha}{r}\right)\phi_{nm} = w_{nm}^1 \qquad (21)$$

The function w_{nm}^1 defines the remainder of the radial expansion,

$$w_{nm}^1(r,t) = \sum_{k=1}^{K} -k\, r^{-k-1-\alpha}\phi_{nm}^k \qquad (22)$$

As noted by Bayliss and Turkel, $w_{nm}^1(r,t) = O(r^{-2})\phi_{nm} = O(r^{-2-\alpha})$. If we set $w_{nm}^1 = 0$, then $B_1\phi_{nm} = 0$. Applying the harmonic expansion to this result evaluated at $r = R$, gives,

$$B_1\phi = 0, \qquad \text{on } \Gamma \qquad (23)$$

which defines the first-order local boundary condition of Bayliss and Turkel.

Applying the local operators L_j, $j = 2, \cdots$ to (22) will reduce the order of the remainder further. In general, applying B_{j+1} to (15), we have by induction,

$$B_{j+1}\phi_{nm} = L_{j+1}(B_j\phi_{nm}) = \left(\frac{1}{c}\frac{\partial}{\partial t} + \frac{\partial}{\partial r} + \frac{2j+\alpha}{r}\right)w_{nm}^j = w_{nm}^{j+1} \qquad (24)$$

with w_{nm}^j defined as,

$$w_{nm}^j(r,t) = \sum_{k=j}^{K} a_k^j\, r^{-k-j-\alpha}\phi_{nm}^k \qquad (25)$$

$$a_k^j = (-1)^j k(k-1)\cdots(k-(j-1)) = (-1)^j \frac{k!}{(k-j)!} \qquad (26)$$

We note, $w_{nm}^j(r,t) = O(r^{-2j})\phi_{nm} = O(r^{-2j-\alpha})$.

For $j = 1, 2, \cdots, l_n$ we eliminate radial derivatives in (24) in favor of a recursive sequence for w_{nm}^j. To this end we rewrite,

$$L_{j+1}(w_{nm}^j) = \left(\frac{1}{c}\frac{\partial}{\partial t} + \frac{\partial}{\partial r} + \frac{2j+\alpha}{r}\right)w_{nm}^j = w_{nm}^{j+1}, \qquad (27)$$

as,

$$\frac{1}{c}\frac{\partial w_{nm}^j}{\partial t} = \frac{1}{2}w_{nm}^{j+1} - \frac{j}{r}w_{nm}^j - \frac{1}{2}\left(\frac{\partial}{\partial r} + \frac{\alpha}{r} - \frac{1}{c}\frac{\partial}{\partial t}\right)w_{nm}^j \qquad (28)$$

Now consider the last term in the brackets,

$$\left(\frac{\partial}{\partial r} + \frac{\alpha}{r} - \frac{1}{c}\frac{\partial}{\partial t}\right)w_{nm}^j = \sum_{k=j}^{K} a_k^j r^{-k-j-\alpha}\left\{2(\phi_{nm}^k)' - (k+j)r^{-1}\phi_{nm}^k\right\} \qquad (29)$$

Substituting the recursion relation for $(\phi_{nm}^k)'$ given in (17), and the definition for a_k^j given in (26), into (29) leads to,

$$\left(\frac{\partial}{\partial r} + \frac{\alpha}{r} - \frac{1}{c}\frac{\partial}{\partial t}\right)w_{nm}^j = -\frac{2j\, c_n^j}{r^2}w_{nm}^{j-1} \qquad (30)$$

Using this key result in (28) defines the following recursive sequence for the functions $w_{nm}^j(r,t)$, $j = 1, 2, \cdots, l_n$:

$$\frac{1}{c}\frac{\partial w_{nm}^j}{\partial t} = \frac{j\, c_n^j}{r^2}w_{nm}^{j-1} - \frac{j}{r}w_{nm}^j + \frac{1}{2}w_{nm}^{j+1} \qquad (31)$$

with $w_{nm}^0 = \phi_{nm}$.

Rescaling the variables by 2^{1-j}, applying the harmonic expansion to (21) and (31), leads to the sequence of local radiation boundary conditions given in Hagstrom and Hariharan (Hagstrom, 1998) involving the tangential derivatives defined in (7). While these conditions can be effectively implemented in a finite difference scheme (Hagstrom, 1998), direct finite element implementation in a standard Galerkin variational equation would result in a nonsymmetric system of equations. To address this difficulty, we recognize that when evaluated on the artificial boundary at $r = R$, the sequence (31) forms a system of first-order ordinary differential equations in time for the auxiliary functions,

$$v_{nm}^j(t) = 2^{1-j} w_{nm}^j(R,t) \tag{32}$$

Here we set $\boldsymbol{v}_{nm}(t) = \{2^{1-j} w_{nm}^j(R,t)\}$, $j = 1, 2, \cdots l_n$, and define a time-dependent vector function of order l_n,

$$\boldsymbol{v}_{nm}(t) = [v_{nm}^1(t), v_{nm}^2(t), \cdots, v_{nm}^{l_n}(t)]^T \tag{33}$$

We then write the system of equations defined by (31) as a first-order matrix differential equation for each harmonic:

$$\frac{d}{dt} \boldsymbol{v}_{nm}(t) = \boldsymbol{A}_n \boldsymbol{v}_{nm}(t) + \boldsymbol{b}_n \phi_{nm}(R,t) \tag{34}$$

with constant $l_n \times l_n$, tri-diagonal matrix $\boldsymbol{A}_n = \{A_n^{ij}\}$,

$$A_n^{ij} = \frac{c}{R} \begin{cases} R & \text{if } i = j - 1 \\ -i & \text{if } i = j \\ i c_n^i / 2R & \text{if } i = j + 1 \\ 0 & \text{otherwise} \end{cases} \tag{35}$$

The constant vector $\boldsymbol{b}_n = \{b_n^j\}$ is defined by:

$$\boldsymbol{b}_n = \begin{cases} \dfrac{(1 - 4n^2)c}{8R^2} \boldsymbol{e}_1, & d = 2 \\ -\dfrac{n(n+1)c}{2R^2} \boldsymbol{e}_1, & d = 3 \end{cases} \tag{36}$$

where $\boldsymbol{e}_1$ is the unit vector,

$$\boldsymbol{e}_1 = [1, 0, \ldots, 0]^T \tag{37}$$

We then define the radiation boundary condition by taking the harmonic expansion of (21) and evaluating on the truncation boundary at $r = R$:

$$\left(\frac{1}{c} \frac{\partial}{\partial t} + \frac{\partial}{\partial r} + \frac{\alpha}{r} \right) \phi = \sum_{n=n_1}^{\infty} \sum_{m=-m_0}^{m_0} v_{nm}^1(t) y_{nm}(\boldsymbol{\theta}), \text{ on } \Gamma \tag{38}$$

where

$$n_1 = \begin{cases} -\infty, & d = 2 \\ 1, & d = 3 \end{cases} \tag{39}$$

In the above, the function $v_{nm}^1(t) = w_{nm}^1(R,t)$ satisfies the Cauchy problem for each harmonic defined by the first-order matrix system (34), with initial condition $\boldsymbol{v}_{nm}(0) = 0$, and driven by the radial modes defined by the harmonic transform,

$$\phi_{nm}(R,t) = \int_{\Gamma} y_{nm}^*(\boldsymbol{\theta}) \phi(R, \boldsymbol{\theta}, t) \, d\Gamma \tag{40}$$

where

$$d\Gamma = \begin{cases} R \, d\theta, & d = 2 \\ R^2 \sin\theta \, d\theta \, d\phi, & d = 3 \end{cases} \tag{41}$$

Here, the star indicates complex conjugate.

In three-dimensions, when the number of functions $v_{nm}^j(t)$ included in the system (34) is equal to the number of harmonics in the solution, i.e. $l_n = n$, then $v_{nm}^{n+1}(t) = 0$, and the boundary condition is exact and is equivalent to the exact nonreflecting boundary conditions derived in (Grote, 1995b; Thompson, 1999a). This result follows from the finite expansion (15), with the index defined over the finite range $k = 0, 1, \cdots, n$. We also note that the auxiliary functions satisfy the property, $v_{nm}^{j+1} = O(R^{-2}) v_{nm}^j$, so that $v_{nm}^{j+1} < v_{nm}^j$, and $v_{nm}^j = O(R^{-2j-\alpha})$. Therefore, if fewer equations are used, i.e. $l_n < n$, then the three-dimensional boundary condition forms a uniform asymptotic approximation to the exact condition. In two-dimensions, the expansion (15) ranges over an infinite number of multipoles, so that for a finite value l_n, the boundary condition also forms a uniform asymptotic approximation. We note several advantages of the radiation boundary condition (38) compared to the nonreflecting boundary conditions derived in (Grote, 1995b; Thompson, 1999a), including a banded tri-diagonal coefficient matrix $\boldsymbol{A}_n$, the avoidance of an additional vector inner product to compute the function $v_{nm}^1(t)$, and the implementation as a uniform approximation to the exact condition, with corresponding reduced memory and computational work.

In practice, the infinite sum over n in (38) is truncated at a finite value N:

$$B_1 \phi = \sum_{n=N_1}^{N} \sum_{m=m_0}^{m_0} v_{nm}^1 y_{nm} \tag{42}$$

5

where

$$N_1 = \begin{cases} -N, & d = 2 \\ 1, & d = 3 \end{cases} \tag{43}$$

For $n > N$, then the boundary condition reverts to the first-order local boundary condition, $B_1 \phi = 0$. To improve the approximation to the truncated harmonics $n > N$, without affecting the modes $n \le N$, we define a modified boundary condition using (24) for $j = 1$, and $r = R$:

$$B_2 \phi = \sum_{n=N_2}^{N} \sum_{m=m_0}^{m_0} 2 v_{nm}^2(t) y_{nm}(\boldsymbol{\theta}), \qquad \text{on } \Gamma \tag{44}$$

where

$$N_2 = \begin{cases} -N, & d = 2 \\ 2, & d = 3 \end{cases} \tag{45}$$

In the above, the function $v_{nm}^2(t) = w_{nm}^2(R,t)/2$ satisfies the same first-order matrix system (34), for each harmonic (40). This modified boundary condition may be implemented in the finite element method using the procedures described in (Thompson, 1999b).

FINITE ELEMENT FORMULATION

In the following, we give the finite element formulation for the initial-boundary value problem within the bounded region Ω, supplemented by the radiation boundary condition (38) on Γ.

Variational Equation

The statement of the weak form for the initial-boundary value problem in the computational domain Ω may be stated as:

Given: f, β_1, β_2, γ, c,
Find: $\phi(\boldsymbol{x}, t)$ in $\Omega \cup \partial\Omega$, such that for all admissible weighting functions $\bar{\phi}$, the following variational equation is satisfied,

$$M(\bar{\phi}, \phi) + C(\bar{\phi}, \phi) + K(\bar{\phi}, \phi) = F_S(\bar{\phi}) + F_\Gamma(\bar{\phi}) \tag{46}$$

with,

$$M(\bar{\phi}, \phi) := \int_\Omega \frac{1}{c^2} \bar{\phi} \frac{\partial^2 \phi}{\partial t^2} \, d\Omega \tag{47}$$

$$C(\bar{\phi}, \phi) := \int_S \frac{\beta_2}{\beta_1} \bar{\phi} \frac{\partial \phi}{\partial t} \, dS + \int_\Gamma \frac{1}{c} \bar{\phi} \frac{\partial \phi}{\partial t} \, d\Gamma \tag{48}$$

$$K(\bar{\phi}, \phi) := \int_\Omega \nabla\bar{\phi} \cdot \nabla\phi \, d\Omega$$
$$+ \int_S \frac{\gamma}{\beta_1} \bar{\phi} \phi \, dS + \frac{\alpha}{R} \int_\Gamma \bar{\phi} \phi \, d\Gamma \tag{49}$$

$$F_S(\bar{\phi}) := \int_\Omega \bar{\phi} f \, d\Omega + \int_S \bar{\phi} \frac{g}{\beta_1} \, dS \tag{50}$$

$$F_\Gamma(\bar{\phi}) := \sum_{n=n_1}^{\infty} \sum_{m=-m_0}^{m_0} v_{nm}^1 \int_\Gamma \bar{\phi} y_{nm} \, d\Gamma \tag{51}$$

In the above, v_{nm}^1 satisfies the system of first-order differential equations (34), driven by the modes $\phi_{nm}(R,t)$ computed from (40). The constant α is defined in (8).

Finite element discretization

To obtain a finite element approximation to the solution of the variational equation (46), the domain $\bar{\Omega}$ is discretized into a finite number of subdomains (elements), and we apply the standard Galerkin semi-discrete approximation,

$$\phi(\boldsymbol{x}, t) \approx \phi^h(\boldsymbol{x}, t) = \boldsymbol{N}(x) \boldsymbol{\phi}(t) \tag{52}$$

where $\boldsymbol{N}(\boldsymbol{x})$ is a row vector of standard C^o basis functions with compact support associated with each node, and $\boldsymbol{\phi}(t)$ is a time-continuous column vector containing the nodal values of ϕ^h. The superscript h denotes a finite-dimensional basis. Using this approximation in (46), we arrive at the following system of second-order ordinary differential equations in time:

$$\boldsymbol{M}\ddot{\boldsymbol{\phi}}(t) + \boldsymbol{C}\dot{\boldsymbol{\phi}}(t) + \boldsymbol{K}\boldsymbol{\phi}(t) = \boldsymbol{F}(t), \qquad t > 0 \tag{53}$$

$$\boldsymbol{\phi}(0) = \boldsymbol{\phi}_o, \qquad \dot{\boldsymbol{\phi}}(0) = \dot{\boldsymbol{\phi}}_o \tag{54}$$

In the above, $\boldsymbol{M}$, $\boldsymbol{C}$, and $\boldsymbol{K}$ are standard banded/sparse arrays associated with the finite element discretization of the wave equation and the local B_1 operator; and $\boldsymbol{F}(t) = \boldsymbol{F}_S + \boldsymbol{F}_\Gamma$ is the discrete force vector composed of a standard load vector $\boldsymbol{F}_S$ and a part associated with the auxiliary functions appearing in the radiation boundary condition:

$$\boldsymbol{F}_\Gamma(t) = \sum_{n=N_1}^{N} \sum_{m=-m_o}^{m} v_{nm,1}^h(t) \, \boldsymbol{f}_{nm} \tag{55}$$

where,

$$\boldsymbol{f}_{nm} := \int_\Gamma \boldsymbol{N}^T(\boldsymbol{\theta}) y_{nm}(\boldsymbol{\theta}) \, d\Gamma \tag{56}$$

In (55), the function $v^h_{nm,1}$ is the first element of the vector array $\boldsymbol{v}^h_{nm} = \{v^h_{nm,j}\}$ which is a solution to the system of first-order differential equations (34) driven by $\phi^h_{nm}(t) = \boldsymbol{f}^{*T}_{nm} \cdot \boldsymbol{\phi}(t)$. The radiation boundary condition only requires inner products of harmonics and finite element basis functions with compact support within the boundary vector $\boldsymbol{f}_{nm}$. As a result, the components of the force vector are easy to compute, either at each node on the radiation boundary Γ, or over each element on the boundary and using standard element vector assembly. We note that the implementation does not disturb in any way the symmetric, and banded/sparse structure of the finite element matrix equations. In practice, for real boundary condition data on S, it may be advantageous to use real instead of complex harmonics. In this case the real harmonic is composed of the real and imaginary parts of (12) with a modified normalization.

Furthermore, the harmonics $y_{nm}(\boldsymbol{\theta})$ may be approximated by a projection onto the finite-dimensional basis. In particular, the harmonics may be approximated by the interpolant of y_{nm}, using the expansion,

$$y_{nm}(\boldsymbol{\theta}) \approx y^h(\boldsymbol{\theta}) = \boldsymbol{N}(\boldsymbol{\theta})\, \boldsymbol{y}_{nm} \qquad (57)$$

where $\boldsymbol{y}_{nm} = \{y_{nm,l}\}$, $l = 1, 2, \cdots, N_\Gamma$, is a vector containing the nodal values of the harmonic defined by (n,m) on Γ, i.e., $y_{nm,l} = y_{nm}(\boldsymbol{\theta}_l)$. Using this expansion in (55) we have,

$$\boldsymbol{F}_\Gamma(t) = \sum_{n=N_1}^{N} \sum_{m=-m_0}^{m} v^h_{nm,1}(t)\, \boldsymbol{M}_\Gamma \boldsymbol{y}_{nm} \qquad (58)$$

where $\boldsymbol{M}_\Gamma$ is the $N_\Gamma \times N_\Gamma$ symmetric matrix,

$$\boldsymbol{M}_\Gamma := \int_\Gamma \boldsymbol{N}^T \boldsymbol{N}\, d\Gamma \qquad (59)$$

This matrix may be diagonalized using nodal (Lobatto) quadrature, so that the the matrix-vector multiply is reduced to an inner-product. For a uniform mesh on Γ, the work in computing the inner products in (55) and (58) can be reduced by an order of magnitude by use of the Fast Fourier Transform (FFT) in two-dimensions, and fast spherical transform algorithms (Mohlenkamp, 1998; Driscoll, 1997) in three-dimensions.

As discussed in (Thompson, 1999a), one time-integration approach is to apply the explicit central difference method directly to (53). This method requires the forcing term $\boldsymbol{F}^k = \boldsymbol{F}(t_k)$ at time step $t_k = k\Delta t$. Therefore, to update the solution $\boldsymbol{d}^{k+1} = \boldsymbol{\phi}(t_{k+1})$, only the evaluation of $\boldsymbol{v}^k_{nm} = \boldsymbol{v}_{nm}(t_k)$ is needed. To numerically solve (34) either the explicit second-order Adams-Bashforth method or the the implicit second-order

Adams-Moulton method (trapezoidal rule) may be used. The computational work required in solving is negligible, since the matrices $\boldsymbol{A}_n$, are banded, relatively small (usually $N \leq 25$), and remain constant. When $l_n < n$, the work is further reduced.

An alternative approach is to apply the Newmark family of algorithms (and variations such as HHT-α) in predictor/corrector form to the semidiscrete equations (53), see (Thompson, 1999a). Any of the members of the Newmark family may be used, including the second-order accurate and unconditionally stable trapezoidal rule, and conditionally stable central difference method. When solving using the explicit central difference method, the equations may be decoupled using standard diagonal mass $\boldsymbol{M}$, and damping matrices $\boldsymbol{C}$, e.g. using nodal quadrature, row-sum technique, or the HRZ lumping scheme. The solution of the Newmark algorithm requires the forcing term $\boldsymbol{F}^{k+1}$, and therefore $\boldsymbol{v}^{k+1}_{nm}$. In this case the value $\boldsymbol{v}^{k+1}_{nm}$, may be computed concurrently using an explicit time-integrator applied to (34); e.g., the explicit second-order accurate Adams-Bashforth algorithm. Complete algorithms for computing the solution concurrently with auxiliary functions on Γ, using either implicit or explicit time-integrators, are given in (Thompson, 1999a).

NUMERICAL EXAMPLES

Numerical examples are performed to study the accuracy of the radiation boundary condition defined in (38). In the following we denote the truncated boundary condition by RBC1(N,P), where N defines the number of terms included in the truncated series, and $P \leq N$ defines the maximum number of equations, included in the Cauchy problem (34). In particular, we define the number of equations l_n, used in (34), for each mode $n \leq N$, to be: $\{l_n = n,$ for $n < P,$ and $l_n = P,$ for $n \geq P\}$.

Transient Radiation from a Piston on a Sphere

Consider time-dependent radiation from a circular piston on a sphere with radius $a = 0.5$, such that

$$\phi(a, \theta, t) = f(\theta) \sin \omega t\, H(t), \qquad 0 \leq \theta \leq \pi \qquad (60)$$

where $H(t)$ is the unit-step (Heaviside) function and,

$$f(\theta) = \begin{cases} 1, & 0^o \leq \theta \leq \theta_1 \\[2mm] \dfrac{\cos\theta - \cos\theta_2}{\cos\theta_1 - \cos\theta_2}, & \theta_1 < \theta \leq \theta_2 \\[2mm] 0, & \text{otherwise} \end{cases} \qquad (61)$$

For this example, we set $\theta_1 = 15^o$, and $\theta_2 = 30^o$. This problem is challenging because the waves radiated at the piston pole
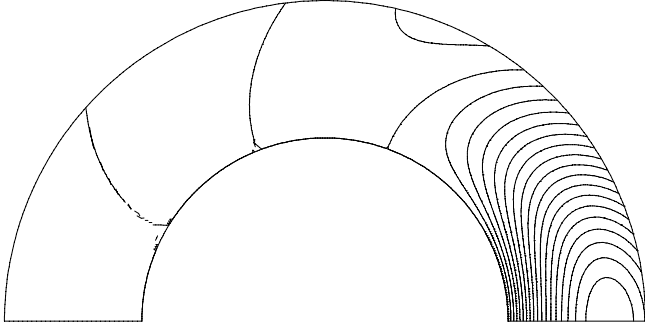
Figure 2. RADIATION FROM A PISTON ON A SPHERE WITH RADIUS $a = 0.5$ AND FREQUENCY $\omega a/c = \pi$. SOLUTION CONTOURS AT STEADY-STATE, USING RBC1(20,20). RADIATION BOUNDARY Γ SET AT $R/a = 1.75$.

Figure 3. TIME-HISTORIES AT OBSERVATION POINT ON $R/a = 1.75$, AND $\theta = \pi$.

$\theta = 0^o$ are attenuated by a geometric spreading loss as they travel along longitudes down to the south pole $\theta = 180^o$.

Since the problem is independent of φ, it is sufficient to compute the solution in the domain Ω defined by the (r,θ) plane for $a \le r \le R$, and $0 \le \theta \le \pi$. The computational domain Ω is discretized with a uniform mesh of standard 4-node bilinear axisymmetric finite elements. The boundary Γ, is positioned at three different locations defined by $R/a = [1.25, 1.5, 1.75]$, with corresponding meshes of $[10, 20, 30] \times 240$ elements evenly spaced in the region $(0.5 \le r \le R) \times (0 \le \theta \le \pi)$. The computation is driven from rest to steady-state with a normalized frequency $\omega a/c = \pi$ and a time step $\Delta t = 0.005$.

For reference, Figure 2 shows contours of the numerical solution using RBC1(20,20) positioned at $R/a = 1.75$, for a representative time $t = 4$, during steady-state. Figure 3 shows the solution at the observation point $R/a = 1.75$ and $\theta = 180^o$. In this difficult region, the solution using B_1 and B_2 exhibits large spurious reflections, while the solution using RBC1(20,20) gives accurate solutions.

The instantaneous error measured in L_2 norm on a spherical boundary with radius $r = R_o$ is defined as,

$$E(t) = \left\{ \int_{\Gamma} \left(\phi^h - \phi \right)^2 d\Gamma \right\}^{1/2} \tag{62}$$

where ϕ^h is the approximate finite element solution and ϕ is the exact steady-state solution. The maximum L_2 error over a steady-state interval $t \in (t_1, t_2)$ is computed from $E_{max} = \max_{t_1 \le t \le t_2} E(t)$.
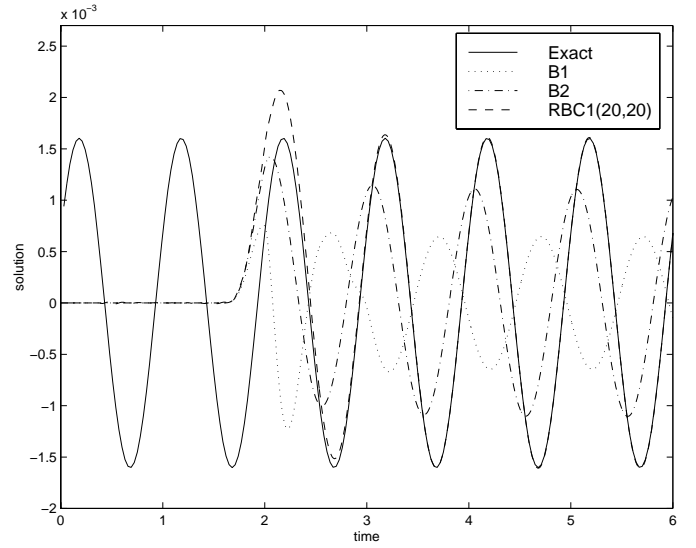
Figure 4 (Top) shows the maximum L_2 error for RBC1(N,N) measured on a sphere with radius $R_o/a = 1.25$, when the radiation boundary condition is moved from $R/a = 1.25$ to $R/a = 1.75$, and N, increasing from 0 to 20. We observe that the solutions using RBC1(N,N) converge to approximately the same minimum error value for each truncation boundary position. This limiting error is controlled primarily by the discretization of the spherical harmonic transforms. With the number of grid points on the boundary, $N_\Gamma = 240$, and $N = 20$, we have $N_\Gamma/N = 12$ angular grid points/mode. As the truncation boundary is moved further away from the source, the number of modes N required to obtain a fixed level of accuracy is reduced. For example, for $R/a = 1.25, N = 20$ terms are needed to converge, whereas, when R/a is increased to 1.75, only $N = 9$ terms are required. Figure 4 (Bottom) shows the maximum error using RBC1(N,P) for fixed $N = 20$, and with variable $P \le 20$. These results show that accurate solutions are obtained using a value of P significantly lower than N, with corresponding reduction in work and memory.

In particular, for the case where the truncation boundary Γ is positioned close to the source ($R/a = 1.25$), such that $N = 20$ modes are needed to obtain accurate solutions, then $P = 5$ is sufficient to converge to the same limiting error value, i.e. the error in RBC1(20,20) $\approx$ RBC1(20,5). The total number of auxiliary equations using the exact condition RBC1(20,20) is 210, while RBC1(20,5) only requires 90 equations, a significant reduction. In general, we observe that $P \ge N/2$ is sufficient to approximate the accuracy of the exact condition.
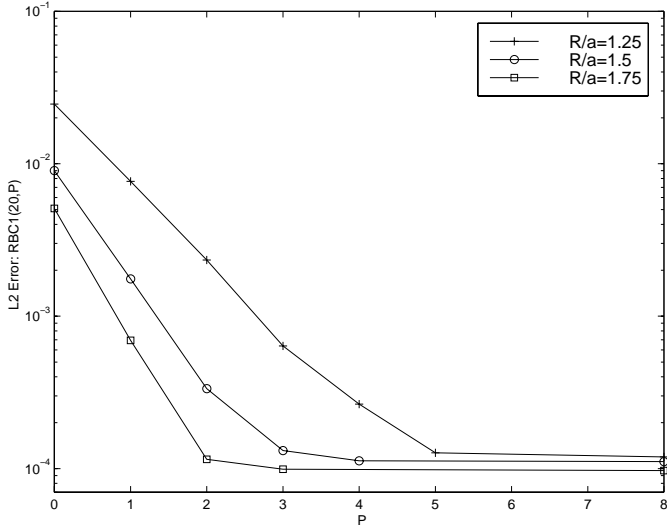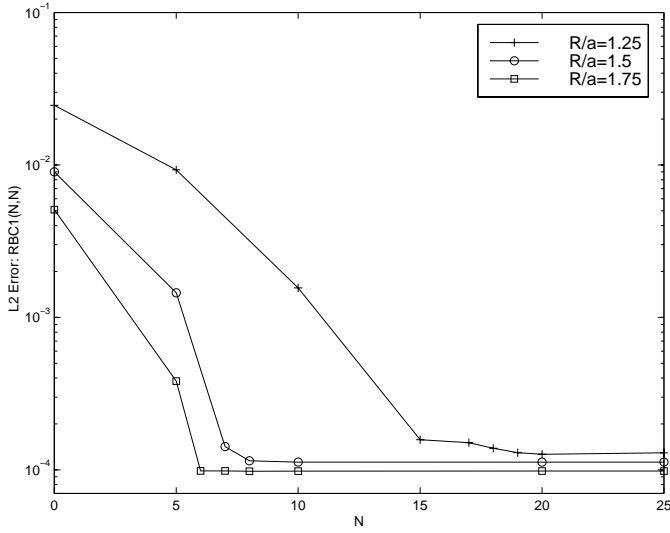
8

Figure 4. RADIATION FROM PISTON ON A SPHERE OF RADIUS $a = 0.5$ AND FREQUENCY $\omega a/c = \pi$. MAXIMUM L_2 ERROR DURING STEADY-STATE MEASURED AT $r/a = 1.25$. RADIATION BOUNDARY CONDITION APPLIED AT TRUNCATION BOUNDARY Γ POSTIONED AT $R/a = 1.25, 1.5, 1.75$. NUMERICAL SOLUTIONS USING (Top): RBC1(N, N), (Bottom): RBC1($20, P$)

Transient Scattering of a Plane Wave by a Cylinder

Consider a cylinder of radius $a = 1$, on which we assume a homogeneous Neumann boundary condition,

$$\frac{\partial \phi}{\partial r} = 0, \qquad \text{on } r = a \qquad (63)$$
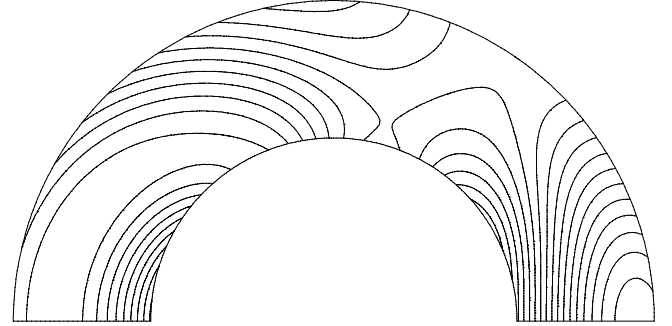
Figure 5. SCATTERING FROM A CYLINDER WITH WAVE INCIDENT FROM THE ($\theta = \pi$) DIRECTION, AND NORMALIZED FREQUENCY $\omega a/c = \pi$. SOLUTION CONTOURS AT STEADY-STATE ($t = 15$), USING RBC1(10,10) AND $R/a = 1.75$

If ϕ is the acoustic pressure, this condition represents a 'rigid' scatterer. Let the incident wave be represented by a traveling plane wave along the z-axis at speed c, i.e.,

$$\phi^{(i)} = \begin{cases} \sin[k(z - z_o) - \omega t], & t \geq \frac{z - z_o}{c} \\ 0, & t < \frac{z - z_o}{c} \end{cases} \qquad (64)$$

Here $k = \omega/c$, and z_o is the location of the plane wave at time $t = 0$. The total field $\phi(r, \theta, t)$ is composed of a superposition of the incident wave $\phi^{(i)}(z, t)$ and a scattered wave $\phi^{(s)}(r, \theta, t)$, i.e. $\phi = \phi^{(i)} + \phi^{(s)}$. With the Neumann boundary condition (63), the scattered field is a solution to the wave equation subject to the boundary condition,

$$\frac{\partial \phi^{(s)}}{\partial r} = -\frac{\partial \phi^{(i)}}{\partial r} = -k \cos u \cos \theta\, H\left(t - \frac{z - z_o}{c}\right), \text{ on } r = a \quad (65)$$

and $u = k(z - z_o) - \omega t$, $z = a \cos \theta$.

The two-dimensional computational domain $\Omega \subset R \subset R^2$, is discretized with a uniform mesh of standard 4-node bilinear finite elements with 240 evenly spaced elements in $0 \leq \theta \leq \pi$. The radiation boundary is placed at three different radii $R/a = [1.25, 1.5, 1.75]$, with corresponding mesh $240 \times [10, 20, 30]$. The computation is driven from rest at $z_o = -2$, to steady-state with a normalized frequency $\omega a/c = \pi$ and a time step $\Delta t = 0.01$.

Contours for the scattered solution computed using RBC1(10,10) positioned at $R/a = 1.75$ are shown in Figure 5. Figure 6 shows time-histories of the scattered solution on the artificial boundary Γ defined by $R/a = 1.25$, and $\theta = 0$. Results are
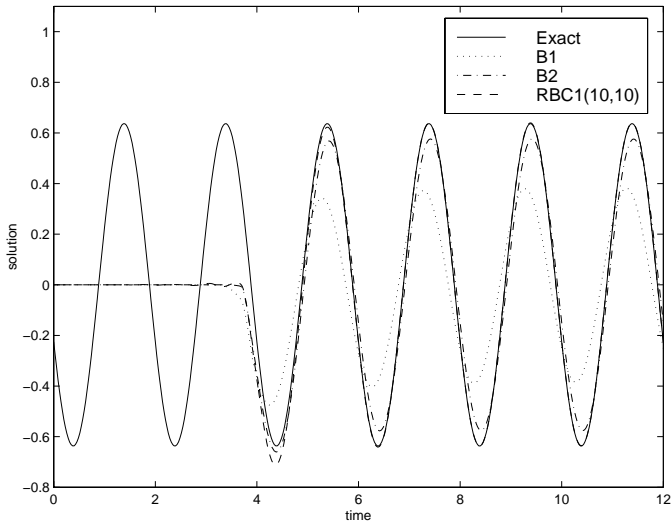
9

Figure 6. SCATTERING OF PLANE WAVE FROM A CYLINDER. TIME-HISTORIES ON THE ARTIFICIAL BOUNDARY Γ, AT $\theta = 0$. RESULTS COMPARED FOR LOCAL OPERATORS B_1, B_2 AND RBC1(N,P) WITH $N = P = 10$.

compared using the local operators B_1, B_2 and RBC1$(10,10)$. At $\theta = 0$, the local operators B_1 and B_2 exhibit significant spurious reflection. In contrast, the solution using RBC1(10,10) matched the exact solution very well.

Figure 7 shows the maximum L_2 error during steady-state measured on a cylinder with radius $R_o/a = 1.25$. For this example, we observe that the solutions using RBC1$(N,10)$ converge rapidly with N. As the radiation boundary is moved further away from the source, the number of modes N required to obtain a fixed level of accuracy is reduced. For $R/a = 1.25$, $N = 8$ modes are needed to converge. As the radiation boundary is moved further away from the scatterer to $R/a = 1.25$, then only $N = 6$ modes are needed. The maximum error using RBC1(N,P) for fixed $N = 8$, and with variable $P \leq 6$, is shown in Figure 7 (Bottom). These results again show that the uniform approximation to the radiation condition is sufficiently accurate with $P \geq N/2$.

CONCLUSIONS

Asymptotic and exact local radiation boundary conditions first derived by Hagstrom and Hariharan for the time-dependent wave equation, are rederived based on the hierarchy of local boundary operators used by Bayliss and Turkel and a recursion relation for the expansion coefficients appearing in the multipole expansion for wave harmonics. With this interpretation, we reformulated the the sequence of local boundary conditions in terms of harmonics and defined a radiation boundary condition (RBC) involving a Cauchy problem for systems of first-order ordinary differential equations for time-dependent auxiliary func-
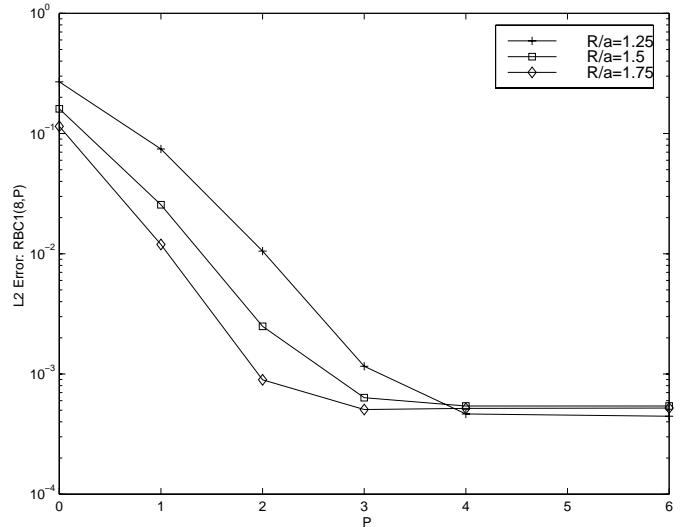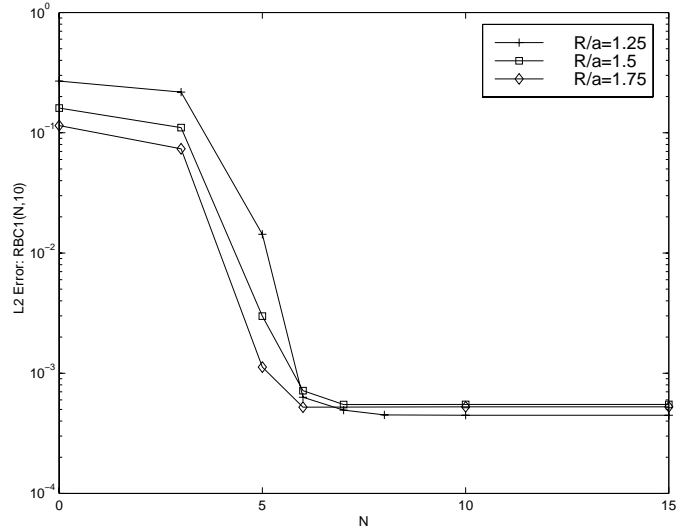

Figure 7. SCATTERING OF A PLANE-WAVE FROM A CYLINDER. MAXIMUM L_2 ERROR DURING STEADY-STATE MEASURED AT $r/a = 1.25$. RADIATION BOUNDARY CONDITION APPLIED AT TRUNCATION BOUNDARY Γ POSTIONED AT $R/a = 1.25$, 1.5, 1.75. NUMERICAL SOLUTIONS USING (Top): RBC1$(N,10)$, (Bottom): RBC1$(8,P)$

tions similar to that used in (Grote, 1995b; Thompson, 1999a). A modified version similar to the formulation given in (Thompson, 1999b) is also reported. The use of harmonics allows the boundary conditions to be implemented concurrently with standard finite element methods without changing the symmetric and banded/sparse structure of the matrix equations.

In three-dimensions, with the number of equations in the Cauchy problem equal to the mode number, this reformulation is exact. If fewer equations are used, then the boundary conditions

form uniform asymptotic approximations to the exact condition. Several improvements over the exact non-reflecting boundary conditions derived in (Grote, 1995b; Thompson, 1999a) have been identified including a banded tri-diagonal coefficient matrix for the auxiliary variables, and reduced memory and computational work needed to store and solve the auxiliary functions for each harmonic. Furthermore, using the approach used to derive the boundary conditions for the sphere, high-order accurate asymptotic RBC's are formulated using Fourier modes for efficient finite element implementation on a circle in two-dimensions.

Numerical studies are performed to assess the accuracy and convergence properties of both the 2D and 3D versions of RBC's. The results demonstrate that the new formulation has dramatically improved accuracy for time domain simulations compared to the first- and second-order local boundary operators of Bayliss and Turkel. Furthermore, for the 3D case, the work in computing the RBC may be reduced using the asymptotic version without significantly impacting accuracy. Further details on the development and formulation of the radiation boundary conditions with several additional numerical examples are reported in (Thompson, 1999d; Huan, 1999) in two- and three-dimensions, respectively, both for individual harmonics, and radiation/scattering problems involving an infinite number of modes.

REFERENCES

S. Tsynkov, 'Numerical solution of problems on unbounded domains. A review', *Appl. Num. Math.* **27**, 465-532, 1998.

J. B. Keller and D. Givoli, 'Exact non-reflecting boundary conditions', *J. Comp. Phys.*, 82 (1989), pp. 172–192.

M. J. Grote and J. B. Keller, 'On nonreflecting boundary conditions', *J. of Comput. Phys.*, 122, 231-243, 1995.

D. Burnett, 'A 3-D acoustic infinite element based on a generalized multipole expansion', *J. Acoust. Soc. Am.*, **96**, (1994), pp. 2798-2816.

R.J. Astley, G.J. Macaulay, J.-P. Coyette, and L. Cremers, 'Three-dimensional wave-envelope elements of variable order for acoustic radiation and scattering. Part I. Formulation in the frequency domain', *J. Acoust. Soc. Am.*, **103**, (1998), pp. 49-63.

A. Bayliss and E. Turkel, 'Radiation boundary conditions for wave-like equations', *Commun. Pure Appl. Math.*, **33**, 707–725, 1980.

P. M. Pinsky and N. N. Abboud, 'Finite element solution of the transient exterior structural acoustics problem based on the use of radially asymptotic boundary operators', *Comput. Methods Appl. Mech. Engrg.* 85 (1991), pp. 311–348.

P. M. Pinsky, L. L. Thompson, and N. N. Abboud, 'Local high-order radiation boundary conditions for the two-dimensional time-dependent structural acoustics problem', *J. Acoust. Soc. Am.* **91** (3), 1992, pp. 1320–1335.

M. J. Grote and J. B. Keller, 'Exact non-reflecting boundary conditions for the time dependent wave equation', *SIAM J. of Appl. Math.*, 55 (1995), pp. 280–297.

M. J. Grote and J. B. Keller, 'Nonreflecting boundary conditions for time dependent scattering', *J. of Comput. Phys.*, 127 (1996), pp. 52–65.

L. L. Thompson and R. Huan, 'Implementation of Exact Non-Reflecting Boundary Conditions in the Finite Element Method for the Time-Dependent Wave Equation', *Computer Methods in Applied Mechanics and Engineering*, to appear, 1999.

H. Lamb, *Hydrodynamics*, Fourth Edition, Cambridge University Press, (1916), p. 517, eq.4.

L. L. Thompson and R. Huan, 'Finite Element Formulation of Exact Non-Reflecting Boundary Conditions for the Time-Dependent Wave Equation', *I. J. for Numerical Methods in Engineering*, to appear, 1999.

L.L. Thompson, and R. Huan, 'Computation of far field solutions based on exact nonreflecting boundary conditions for the time-dependent wave equation', *Computer Methods in Applied Mechanics and Engineering*, to appear, 1999.

T. Hagstrom and S. Hariharan, 'A formulation of asymptotic and exact boundary conditions using local operators', *Appl. Num. Math.* **27**, 403-416, 1998.

M.J. Mohlenkamp, 'A fast transform for spherical harmonics', Accepted August 1998 by *The Journal of Fourier Analysis and Applications*.

J. Driscoll, D. Healy and D. Rockmore, 'Fast discrete polynomial transforms with applications to data analysis for distance transitive graphs', *SIAM J. Comp.*, **26**, 1066 - 1099, 1997.

L.L.Thompson and R. Huan, 'Accurate radiation boundary conditions for the two-dimensional wave equation on unbounded domains', Submitted: 1999.

R. Huan and L.L.Thompson, 'Accurate radiation boundary conditions for the time-dependent wave equation on unbounded domains', Submitted: 1999.